IP-10 induces dissociation of newly formed blood vessels

Richard J. Bodnar[1,2,*], Cecelia C. Yates[2], Margaret E. Rodgers[1], Xiaoping Du[3] and Alan Wells[1,2]

[1]Pittsburgh Veterans Affairs Medical Center, Pittsburgh, PA 15240, USA
[2]Department of Pathology, University of Pittsburgh, Pittsburgh, PA 15261, USA
[3]Department of Pharmacology, University of Illinois, Chicago, IL 60612, USA
*Author for correspondence (e-mail: rjb8@pitt.edu)

Accepted 16 March 2009
Journal of Cell Science 122, 2064-2077 Published by The Company of Biologists 2009
doi:10.1242/jcs.048793

Summary

The signals that prune the exuberant vascular growth of tissue repair are still ill defined. We demonstrate that activation of CXC chemokine receptor 3 (CXCR3) mediates the regression of newly formed blood vessels. We present evidence that CXCR3 is expressed on newly formed vessels in vivo and in vitro. CXCR3 is expressed on vessels at days 7-21 post-wounding, and is undetectable in unwounded or healed skin. Treatment of endothelial cords with CXCL10 (IP-10), a CXCR3 ligand present during the resolving phase of wounds, either in vitro or in vivo caused dissociation even in the presence of angiogenic factors. Consistent with this, mice lacking CXCR3 express a greater number of vessels in wound tissue compared to wild-type mice. We then hypothesized that signaling from CXCR3 not only limits angiogenesis, but also compromises vessel integrity to induce regression. We found that activation of CXCR3 triggers μ-calpain activity, causing cleavage of the cytoplasmic tail of β3 integrins at the calpain cleavage sites c'754 and c'747. IP-10 stimulation also activated caspase 3, blockage of which prevented cell death but not cord dissociation. This is the first direct evidence for an extracellular signaling mechanism through CXCR3 that causes the dissociation of newly formed blood vessels followed by cell death.

Supplementary material available online at
http://jcs.biologists.org/cgi/content/full/122/12/2064/DC1

Key words: Wound healing, Angiogenesis, Chemokines, Endothelial cells, Integrin

Introduction

Regulation of the vascular tree is critical to organogenesis and the 'neo-organogenesis' that occurs during wound repair. While many of the factors that initiate vascular growth are known, little has been deciphered about those that lead to subsequent involution or regression. Three possibilities, none mutually exclusive, have been forwarded: 'disuse atrophy' from mechanical factors secondary to decreasing metabolic load, decrease in pro-angiogenic factors, and actual pro-involution signals (Davis and Saunders, 2006; Lobov et al., 2005; Nyberg et al., 2005). This last possibility has been the least probed. Here, we propose that CXC chemokine receptor 3 (CXCR3) ligands serve as active signalers of vascular regression, at least during skin wound repair.

Early in the dermal wound healing process, the generation of new blood vessels is required for the regeneration of tissue. However, during the regenerative phase of wound healing, angiogenesis stops, followed by involution during the remodeling phase as the metabolic needs decrease in mature skin. Two extracellular signaling factors that appear transiently towards the end of the regenerative phase and into the resolving phase are the ELR-negative CXC chemokines CXCL11 (IP-9, also known as ITAC) and CXCL10 (IP-10; interferon-inducible protein-10) (Yates et al., 2008). These chemokines commonly bind and activate CXCR3, which is expressed on human microvascular endothelial cells. Recently identified, CXCR3-B, a seven transmembrane G-protein-coupled receptor, was found to be the only isoform expressed on endothelial cells (Lasagni et al., 2003). Interestingly, IP-10 and CXCL4 (also known as Platelet Factor 4, PF4) have been reported to be angiostatic (Lasagni et al., 2003; Struyf et al., 2007). We found that signaling through CXCR3 limits angiogenesis both in vitro and in vivo (Bodnar et al., 2006), even overcoming angiogenesis driven by exogenous vascular endothelial growth factor (VEGF), but this does not necessarily lead to vascular regression.

The CXCR3 signaling system is active just prior to and during the stage of vascular regression, making it a viable candidate as an inducer of this second event as well. This hypothesis derives from multiple lines of evidence: First, ligand binding to CXCR3 can actuate μ-calpain activation triggered by phospholipase Cβ and can activate PKA (Bodnar et al., 2006; Satish et al., 2005). Second, μ-calpain has been shown to cleave the terminus of the cytoplasmic tail of, and thereby abrogate signaling through a key endothelial cell integrin, integrin β3 (Xi et al., 2003); this would destabilize newly formed capillaries. Third, in mice lacking CXCR3 (Hancock et al., 2000), skin wound repair is characterized by excessive dermal vascularity (Yates et al., 2007) though this may be due to failure to limit angiogenesis as much as by the lack of vascular involution. These data suggest that CXCR3 signaling contributes to vascular involution. Herein, we demonstrate that CXCR3 ligands induce the regression of newly formed cords and even endothelial cell death in vitro, and loss of blood vessels in vivo. We define a signaling pathway in microvascular endothelial cells from CXCR3, via μ-calpain, to cleavage of integrin β3 and activation of caspase 3 that underlies vascular involution.

Results

IP-10 induces the dissociation of newly formed vessels

Published data (Feldman et al., 2006; Yao et al., 2002) led us to hypothesize that CXCR3 ligands could cause regression of newly formed vessels. For this to occur, the receptor needed to be present

on these vessels because there are reports of CXCR3 being downregulated once endothelial cells are no longer proliferative (Romagnani et al., 2001). To verify that CXCR3 is expressed in vivo, we looked at whether newly formed vessels expressed CXCR3. Growth factor reduced (GFR)-Matrigel supplemented with vascular endothelial growth factor A (VEGF-A) was injected subcutaneouly into the groin area of mice and incubated. Over a 10-day period, blood vessels invaded into the Matrigel; these were competent because erythrocytes were readily detected within them (data not shown). The Matrigel was removed, embedded in paraffin and immunostained for endothelial cells (VECAM-1) and CXCR3. The newly formed vessels within the Matrigel plug expressed CXCR3 (Fig. 1A). CXCR3 was also highly expressed on dermal endothelial cell tubes in an in vitro Matrigel assay (supplementary material Fig. S2).

To determine whether CXCR3 expression occurs under physiological conditions, mice underwent full thickness excisional wounding. At various time points, biopsies were taken, embedded in paraffin, and immunostained for endothelial cells (von Willebrand factor, vWF) and CXCR3. Endothelial cells (stained red in Fig. 1B) in unwounded tissue showed little or no CXCR3 (stained green in Fig. 1B) but newly formed vessels found in the wound bed (day 7 and 14) showed significant CXCR3 staining. The extensive CXCR3 staining on cells lacking vWF observed at days 7 and 14 marks the inflammatory cell infiltrate and fibroblast invasion into the wound bed; these cells have been shown to express CXCR3 (Kouroumalis et al., 2005; Tsubaki et al., 2005). By day 21, the level of CXCR3 had decreased, and by day 30, when the wound was considered healed, CXCR3 staining was almost undetectable on vessels. These results indicate that during the angiogenic process newly forming vessels express CXCR3 and that, upon maturation, these vessels no longer express CXCR3. This situation is supportive of our hypothesis in that CXCR3 is in the right place at the right time.

To examine whether vessel regression might be driven by CXCR3 signaling in a physiological context, wound repair was probed in mice deficient in CXCR3 (Hancock et al., 2000; Yates et al., 2007) (Fig. 2A). During wound healing there is a significant ingrowth of vessels into the wound tissue, which regress during the remodeling phase and leave the dermis relatively avascular. Interestingly, during this later period there is an increase in ELR-negative chemokines (Yates et al., 2007). Analysis of the vascularity of *CXCR3*$^{-/-}$ and wild-type wounds at days 14 and 30 post-wounding showed a significant increase in the number of vessels observed in the *CXCR3*$^{-/-}$ mice compared to wild-type mice (Fig. 2B). Although the number of vessels does diminish over time, as there are probably redundant mechanisms (Yates et al., 2007), CXCR3-deficient mice still present a more vascular wound bed. These results suggest, though do not directly demonstrate, that the ERL-negative chemokines (PF4, IP-10, IP-9 and Mig), ligands for CXCR3-B, can

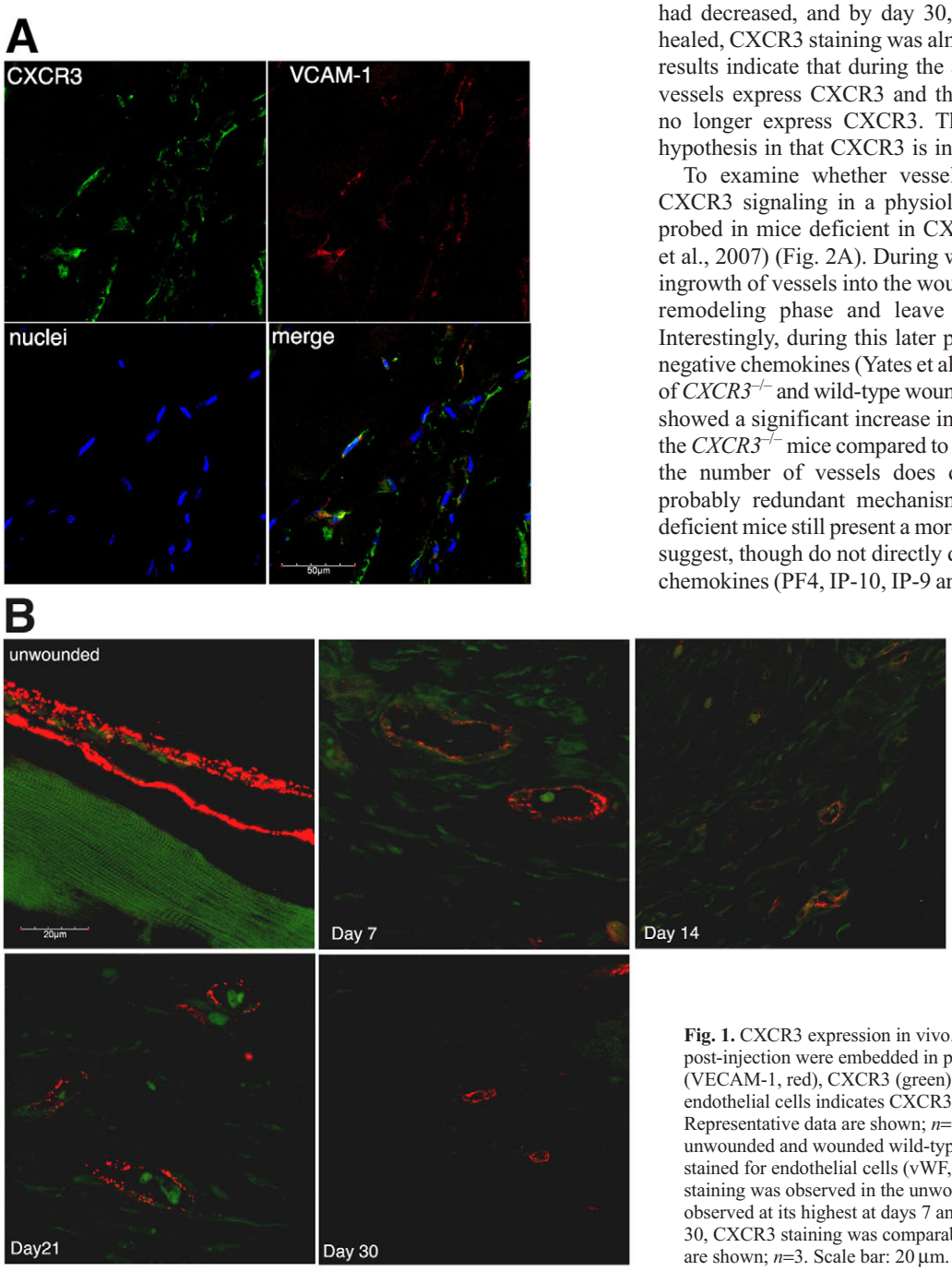

Fig. 1. CXCR3 expression in vivo. (A) Matrigel plugs extracted 10 days post-injection were embedded in paraffin and stained for endothelial cells (VECAM-1, red), CXCR3 (green) and nuclei (blue). Green staining of the endothelial cells indicates CXCR3 is expressed on newly formed vessels. Representative data are shown; n=6. Scale bar: 50 μm. (B) Biopsies from unwounded and wounded wild-type mice were embedded in paraffin and stained for endothelial cells (vWF, red) and CXCR3 (green). Little CXCR3 staining was observed in the unwounded vessels. CXCR3 expression was observed at its highest at days 7 and 14 then decreased at day 21. By day 30, CXCR3 staining was comparable to unwounded. Representative data are shown; n=3. Scale bar: 20 μm.

directly induce vessel regression and that CXCR3-B is, at least in part, responsible for mediating vessel regression in wound repair.

The long time-period of in vivo changes may be related to numerous other effects and does not demonstrate direct vessel regression due to CXCR3 activation. We had shown previously that IP-10 could prevent initial angiogenesis when present during the endothelial cell proliferative and migratory phases (Bodnar et al., 2006), but vessel regression is a distinct process occurring after these processes end. To determine whether IP-10 can mediate vessel regression in vivo, GFR-Matrigel loaded with VEGF-A was injected into the subcutaneous space of mice. At 10 and 12 days after implantation, murine IP-10 or saline (the diluent for IP-10) was

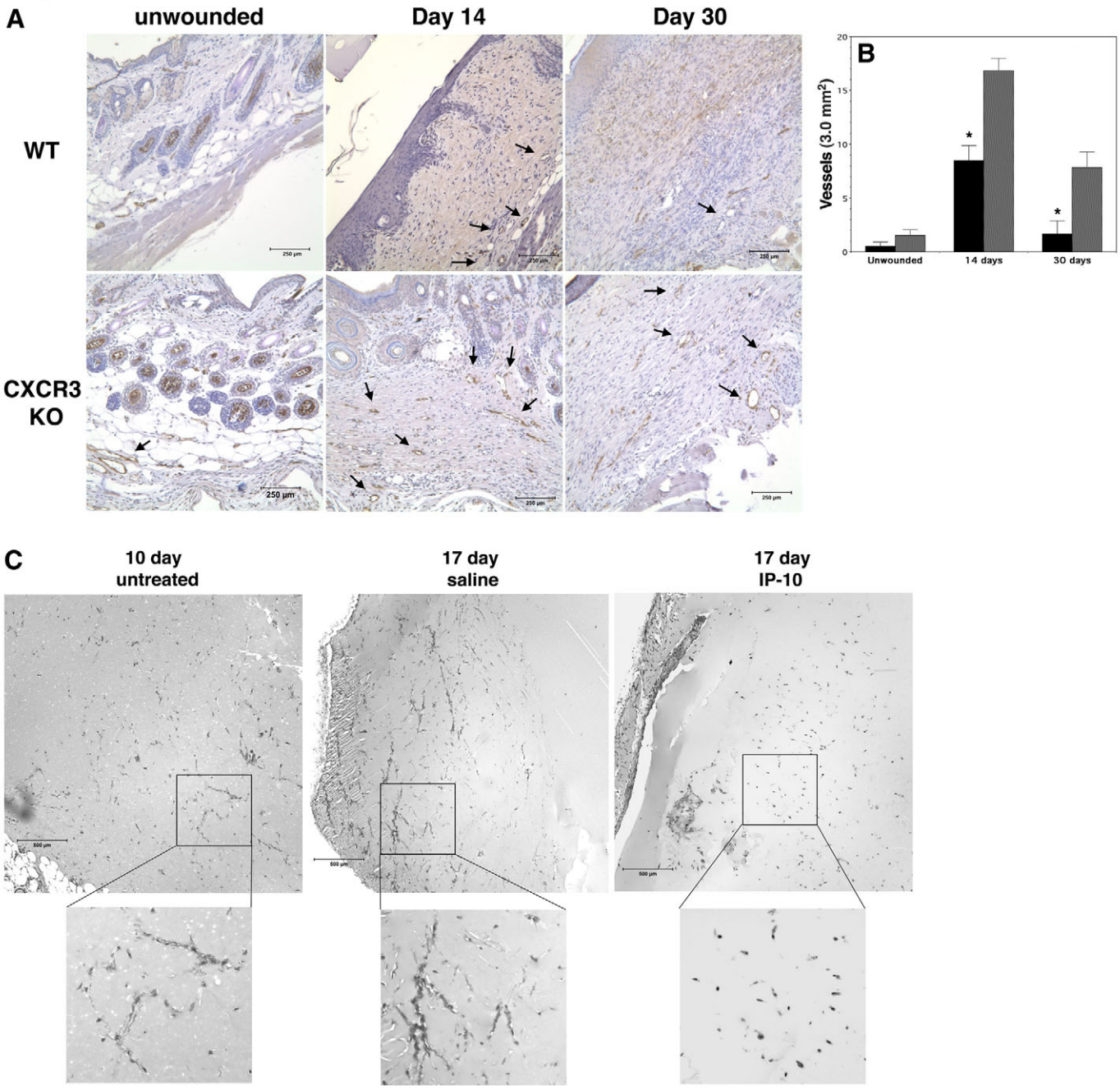

Fig. 2. IP-10 induces in vivo vessel regression. (A) Wound biopsies from wild-type (WT) and CXCR3$^{-/-}$ (CXCR3 KO) mice were immunostained for vWF. In unwounded tissue, very few vessels are observed in either the WT or CXCR3 KO mice. Following wounding there is a greater number of vessels observed in the CXCR3 KO mice at day 14 and 30 compared to WT. Scale bar: 250 μm. (B) Quantitative analysis of the number of vessels in A. The CXCR3 KO mice at day 14 have a twofold increase and at day 30 have a threefold increase in vessels compared to WT. Solid bars, WT mice; hatched bars, CXCR3 KO. Values are mean ± s.e.m. This suggests that CXCR3 plays a role in regulating vascular regression during the wound-healing process. (C) VEGF-A (150 ng/ml) supplemented GFR-Matrigel was injected into the groin of mice. After 10 days the Matrigel was removed (control, n=3) to show vessel invasion (10 days). For the remaining mice (n=10), one side was injected with mIP-10 (5 μg) at days 10 and 12. The other side was treated with an equal volume of saline (diluent). At day 17, the Matrigel was removed and stained with Masson's trichrome to identify vessels. Treatment with IP-10 (17 day IP-10) shows a significant regression of vessels compared to saline control (17 day saline). These data indicated that IP-10 is able to directly cause vessel regression. Representative data are shown; n=3. Scale bar: 500 μm.

injected into the same region as the Matrigel implant. Seven days after initial IP-10 treatment, significantly fewer vessels were observed compared to the saline-treated side (Fig. 2C), a finding consistent with those in tumor angiogenesis (Struyf et al., 2007; Yang and Richmond, 2004). Regression was unlikely to be due to depletion of angiogenic factors because the Matrigel was supplemented with VEGF-A and vessels were more advanced in the saline-treated side (Fig. 2C; 17 days saline).

An in vitro assay for cord or tube formation was used to determine whether ELR-negative CXC chemokines, IP-10 and PF4 (CXCL4) were able to directly induce cord dissociation. Human dermal microvascular endothelial cells (HMEC-1) were incubated on GFR-Matrigel for 24 hours in the presence of VEGF-A or bFGF to promote cord or tube formation, then treated with IP-10, PF4, an unrelated chemokine (IL-8) or diluent for a further 24 hours; the angiogenic factors remained in the media during the entire incubation (Fig. 3A,B). Both IP-10 and PF4, the two ligands that bind CXCR3B avidly (Lasagni et al., 2003), induced dissociation of the endothelial cords, and these were dominant over VEGF-A or bFGF (Fig. 3A,B). IL-8 [having similar structural homology to IP-10 but not a CXCR3 ligand (Booth et al., 2002)] was unable to induce dissociation (Fig. 3A,B). Treatment of formed tubes with IP-9 (CXCL11) did not cause significant tube dissociation (supplementary material Fig. S3); this was not unexpected as IP-9 has a low affinity for the CXCR3B isoform expressed on endothelial cells (Lasagni et al., 2003). Primary adult dermal and lung microvascular endothelial cells presented similar results (Fig. 4). Interestingly, cords formed by human umbilical vein endothelial cells (HUVEC) did not dissociate in the presence of IP-10 (Fig. 4A). This is probably due to negligible expression of CXCR3 in these cells (Salcedo et al., 2000), which is near background, whereas the other endothelial cells all express similarly high levels (Fig. 4B; supplementary material Fig. S4). To demonstrate that this regression is due to CXCR3 signaling, addition of neutralizing antibodies to IP-10 or CXCR3 prevented cord dissociation (Fig. 5). This suggests that activation of CXCR3 mediated cord dissociation.

CXCR3 signaling activates μ-calpain in endothelial cells

As vessel dissociation resembles a detachment phenomenon, we looked at whether calpain-mediated events might be involved. It has been shown that μ-calpain clips the main β3-integrin subunit in endothelial cells (Xi et al., 2003), leading to lessened adhesiveness (Flevaris et al., 2007). Further, CXCR3 signaling can activate μ-calpain in keratinocytes, resulting in lessened adhesiveness (Satish et al., 2005). Using a membrane-permeable synthetic calpain substrate recognized by both m- and μ-calpain, Boc-LM-CMAC (BOC), we find that IP-10 induced calpain activity in dermal

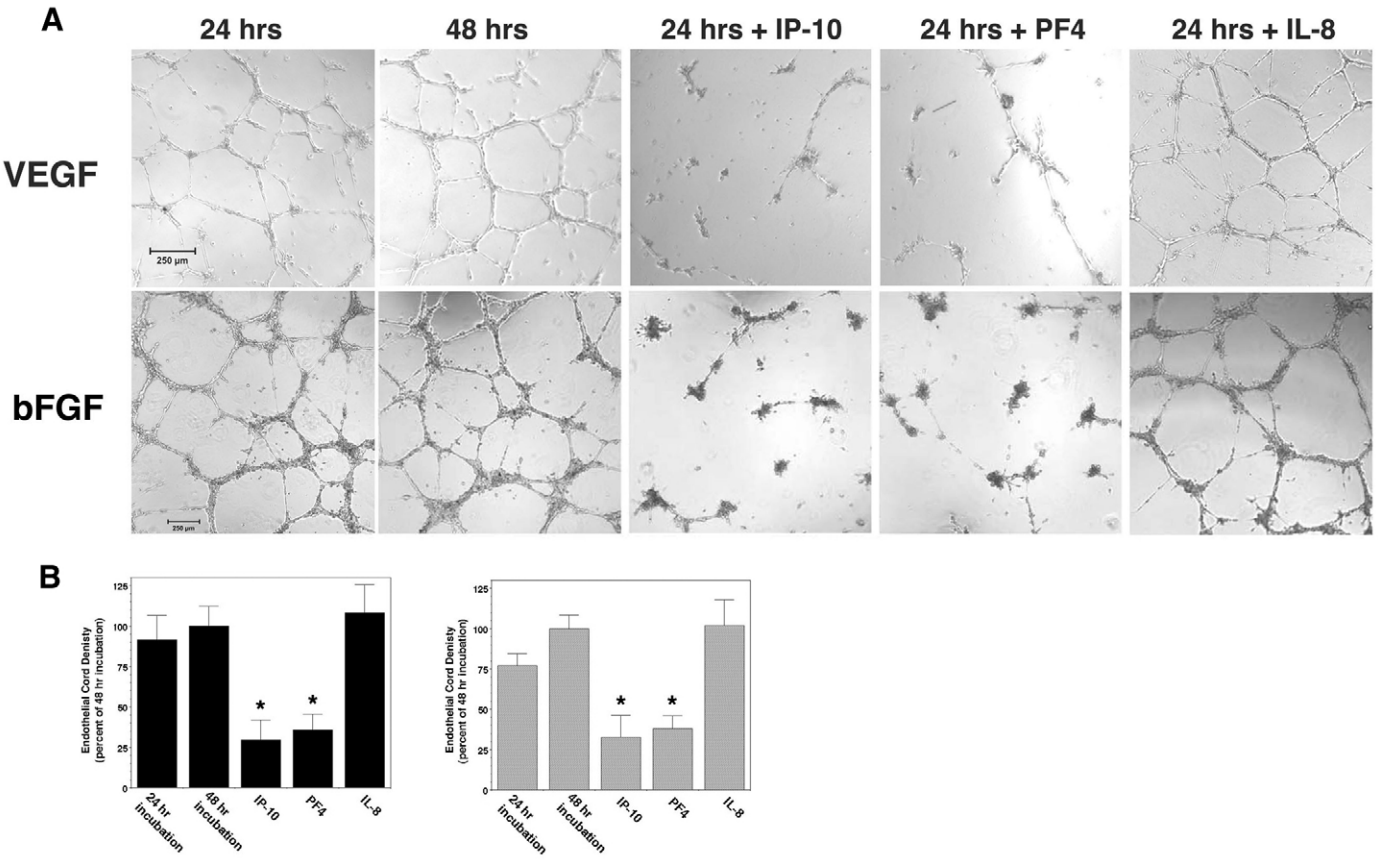

Fig. 3. IP-10 mediates in vitro cord dissociation. (A) HMEC-1 cells treated with VEGF-A (75 ng/ml) or bFGF (50 ng/ml) were plated on GFR-Matrigel to form cords. The cords were incubated in 0.5% dialyzed FBS media for 24 hours with VEGF-A or bFGF (48 hrs) in the presence of IP-10 (600 ng/ml) (24 hrs+IP-10), PF4 (400 ng/ml) (24 hrs+PF4) or IL-8 (100 ng/ml) (24 hrs+IL-8). IP-10 and PF4 caused dissociation of formed cords in the presence of both VEGF and bFGF. Representative data are shown; n=4. Scale bar: 250 μm. (B) Quantification of the endothelial cord area was determined, using MetaMorph. A significant decrease in endothelial cords was observed when treated with IP-10 and PF4. The 48 hour treatment was used as the base line and set at 100%, with the other treatments set as a percentage. Gray bars, VEGF-A-treated; solid bars, bFGF-treated. Values are mean ± s.e.m., n=4 performed in triplicate, *P<0.05 paired Student t-test.

microvascular endothelial cells (Fig. 6A,B). This increase in fluorescence due to BOC cleavage is calpain-mediated as the pan-calpain inhibitor CI-I (ALLN) virtually eliminated fluorescence. In cells, m-calpain is activated, at least in part, by ERK phosphorylation on serine 50 of m-calpain (Glading et al., 2004), and μ-calpain is activated secondary to a calcium flux (Satish et al., 2005). We used BAPTA/AM, a membrane-permeable calcium chelator, to distinguish between m- and μ-calpain activation. Pre-incubation of HMEC-1 cells with BAPTA/AM prevented IP-10-induced BOC cleavage by 75%, compared to IP-10 alone (Fig. 6B). Similar results were also observed in adult dermal human microvascular endothelial cells (dHMEC) (data not shown). We had shown earlier that BAPTA/AM did not block growth-factor-mediated m-calpain activation (Bodnar et al., 2006), thus confirming the specificity of IP-10 activation of μ-calpain. Inhibition of calpain activation by a PLC inhibitor (Et-18-OCH3) suggested that calcium release for μ-calpain activation is mediated via CXCR3 activation of PLC, similar to the activation in keratinocytes (Satish et al., 2005). Furthermore, IP-10 did not induce a change in μ-calpain expression (supplementary material Fig. S6). These data provide evidence suggesting that IP-10 activates μ-calpain in dermal microvascular endothelial cells, providing a potential pathway to endothelial cell retraction and detachment.

μ-Calpain activation leads to vessel dissociation

As μ-calpain contributes to numerous cell functions, we needed to verify its role in vessel regression. HMEC-1 cells formed cords in Matrigel in the presence of VEGF-A, prior to a further 24 hour incubation with IP-10 or A23187 (the calcium flux directly activates μ-calpain) in the presence or absence of CI-1, a pan-calpain inhibitor, Calpain Inhibitor IV (selective for m-calpain), or BAPTA/AM (selective for μ-calpain compared to m-calpain). CI-1 blocked cord dissociation induced by IP-10 or A23187 demonstrating that this dissociation was due to calpain activity (Fig. 7). CI-1 blockade of IP-10 and A23187 cord dissociation was also observed in lung microvascular endothelial cells (data not shown). The calpain isoform was designated by the fact that the m-calpain selective inhibitor CI-IV failed to prevent this dissociation while BAPTA/AM significantly inhibited the IP-10- and A23187-mediated cord dissociation (Fig. 7). The dissociation observed by IP-10 is not as great as in Fig. 3B, which is most likely due to varying experimental conditions, but is still significant. What is more important is that BAPTA/AM and CI-1 are able to significantly inhibit IP-10 mediated cord dissociation and significantly reduce A23187 dissociation. These data suggest that μ-calpain plays a role in endothelial cord dissociation.

IP-10 stimulation results in cleavage of β3 integrin

Activation of μ-calpain leads to proteolytic processing of a number of proteins in the focal adhesion complex (Perrin and Huttenlocher, 2002), including the main integrin subunit in endothelial cell attachment, β3 integrin (Xi et al., 2003; Xi et al., 2006). μ-Calpain has been mapped to cleave at specific NPLY sites in the cytoplasmic domain of β3 integrin (Xi et al., 2006). Cleavage of β3 integrin at Y^{759} inhibited cell spreading and stable adhesion; cleavage at residues F^{754} and Y^{747} completely abolished integrin activation (Xi et al., 2003) and might disrupt VEGF receptor signaling (Mahabeleshwar et al., 2007). Here, we show that IP-10 triggers cleavage of β3 integrin principally at residue Y^{747}, with minor cleavage at F^{754} (Fig. 8). This was observed in both cords (Fig. 8A) and confluent HMEC-1 monolayers (Fig. 8B). Treatment of the

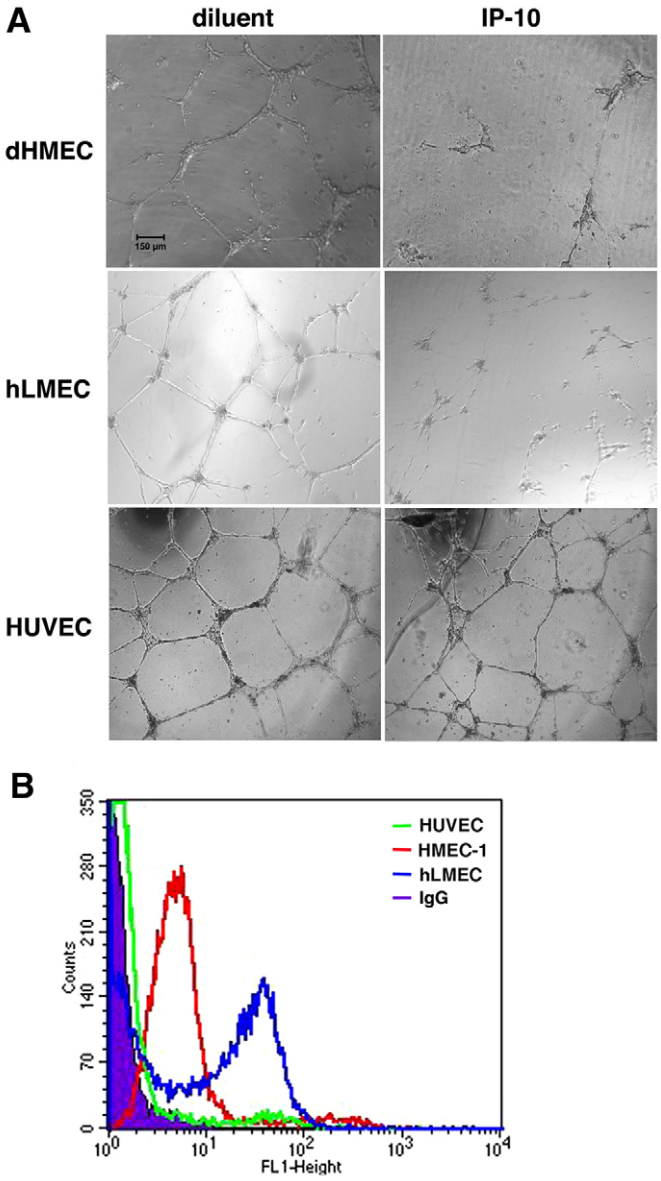

Fig. 4. CXCR3 expression is necessary for IP-10-mediated tube dissociation. (A) dHMEC (passage 5-7), hLMEC (passage 5-7), and HUVEC (passage 3-6) were plated on GFR Matrigel in 2.0% dialyzed dFBS-EGM-2 media containing VEGF (75 ng/ml) and incubated for 24 hours to allow cord formation. The media was removed and the cells incubated in 0.5% dialyzed FBS-EGM-2 media containing VEGF (75 ng/ml) and IP-10 (600 ng/ml) then incubated for 24 hours. IP-10 was able to cause cord dissociation in dHMEC and hLMEC similar to that observed in HMEC-1. Dissociation was not observed in HUVEC. The cords were imaged with a Spot RT_{KE} camera on an Olympus IX 70 microscope (UPlanFl 4×, 0.13). Scale bar: 150 μm. (B) It has been shown that HUVEC had a significantly lower expression of CXCR3 than microvascular endothelial cells (Salcedo et al., 2000). To verify whether the inability of IP-10 to mediate cord dissociation in HUEVCs correlated with low CXCR3 expression in these cells. HMEC-1, hLMEC and HUVEC were detached and fixed in 2% formaldehyde-Hank's balanced salt solution. The cells were incubated with anti-CXCR3 antibody conjugated with FITC and then analyzed on a BD FACSCalbur flow cytometer. The data indicate that CXCR3 expression on HUVEC (green) was just slightly above non-specific IgG (solid graph). Both HMEC-1 (red) and hLMEC (blue) had a high level of cell surface expression of CXCR3. These data suggest that the inability of IP-10 to induce HUVEC tube dissociation is due to the low surface expression of CXCR3.

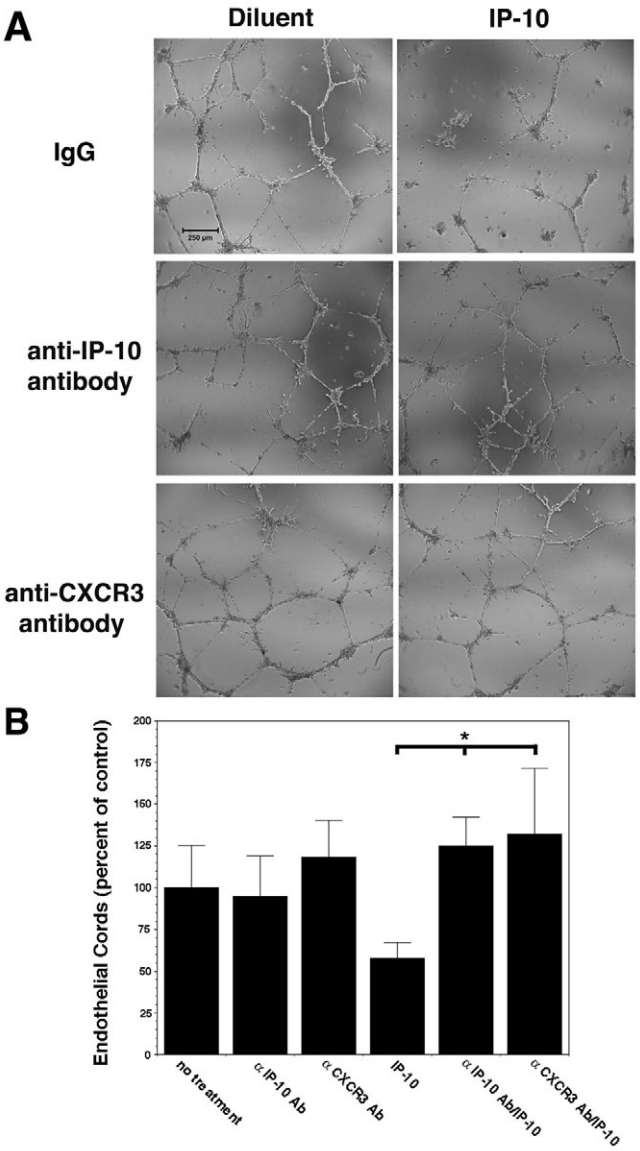

Fig. 5. CXCR3 and IP-10 neutralizing antibody inhibits IP-10-mediated cord dissociation. (A) To verify that IP-10 binding to CXCR3 mediates cord dissociation, formed cords were pretreated with neutralizing antibody to CXCR3 (0.5 μg/ml) 30 minutes prior to addition of IP-10 (600 ng/ml) and incubated for 24 hours. Also, IP-10 (600 ng/ml) was pre-incubated with an IP-10 neutralizing antibody (10 μg/ml) for 30 minutes prior to incubation with formed cords. As seen, both CXCR3 and IP-10 neutralizing antibodies were able to inhibit IP-10-mediated cord dissociation, indicating that IP-10 is responsible for in vitro cord dissociation. The figures are representative of three individual experiments performed in triplicate. Scale bar: 250 μm. (B) Quantification of the endothelial cords, using MetaMorph shows that neutralizing antibodies to CXCR3 and IP-10 significantly inhibit IP-10-mediated cord dissociation. The base line, untreated cords (no treatment), was set at 100% and the other treatments are stated as a percentage of the control. Values are mean ± s.e.m., n=3 performed in triplicate, *P<0.05 paired Student t-test.

cords with the ionophore, A23187, which directly activates μ-calpain, also showed a similar staining to that of IP-10 (Fig. 8A). Furthermore, this cleavage also occurs in confluent cell culture (Fig. 8B). The decrease in immunoreactivity of the c'762 antibody (full length) indicates cleavage of the cytoplasmic domain of β3 integrin. An increase in staining of the c'754 and c'747 antibodies indicates cleavage of β3 integrin at these specific residues (Fig. 8B). Cleavage of β3 integrin at Y^{759} was not observed (data not shown).

To determine whether this integrin cleavage was secondary to μ-calpain, the cells were pretreated with BAPTA/AM, CI-1 or Et-18-OCH3 prior to IP-10 incubation. Immunoreactivity by the antibody recognizing the full-length C-terminal domain increased, indicating that these inhibitors blocked IP-10-mediated cleavage of β3 integrin compared to IP-10 alone (Fig. 8C). As expected, BAPTA/AM (but not ET-18-OCH3) was able to limit the A23187-mediated cleavage of β3 integrin (Fig. 8C); the potency of A23187 activation precludes complete suppression by BAPTA/AM. That μ-calpain cleaved β3 integrin was shown by preventing the cleavage of β3 integrin by blocking any one of the three major steps in the CXCR3 signaling cascade to μ-calpain activation (Satish et al., 2005). Inhibitors of PLCβ (Et-18-OCH3), calcium flux (BAPTA/AM) or calpain (CI-I) prevented IP-10-induced loss of full length β3 cleavage (Fig. 8C). Taken together, these data indicate that calpain is responsible for IP-10-induced cleavage of β3 integrin.

IP-10 causes endothelial cell death

Whether cell death is a cause or an effect of vessel regression is still debated (Jimenez et al., 2000; Rehn et al., 2001; Tarui et al., 2001). Herein, we provide data showing that activation of the death pathway (via caspase 3) lags behind that of β3 integrin cleavage, suggesting that cell death is a consequence of integrin cleavage. In endothelial cells, cleavage of β3 integrin by μ-calpain is associated with caspase-3-mediated cell death (Meredith et al., 1998). We wanted to determine whether IP-10-induced vessel regression requires cell death. Endothelial cords were incubated with IP-10, A23187 or camptothecin (a chemotherapeutic agent that activates caspase 3) then analyzed for activation of caspase 3. HMEC-1 cords in Matrigel were incubated with IP-10, A23187 or camptothecin for 4-36 hours. The cells were fixed, permeabilized and then stained for activated caspase 3 (green) and propidium iodide (PI, red) to show nuclei (Fig. 9). Only a minor fraction of the cells stained positive for activated caspase 3 at 24 hours when treated with IP-10, whereas significant staining was observed at 36 hours (Fig. 9). Treatment with A23187 showed activation of caspase 3 as early as 12 hours, with significant caspase 3 activity by 36 hours. Although not definitively establishing a cause-and-effect connection, the fact that the greater part of caspase activation occurs after 24 hours, whereas we note cord dissociation for IP-10 treatment within 12-24 hours, argues strongly that it is only after endothelial cells dissociate that cell death ensues.

Vessel regression is independent of cell death

We examined whether endothelial death was necessary for cord dissociation or whether there might be a secondary event to remove the cells after the nascent vessels involute. The data above indicate that dissociation, through cleavage of β3 integrins and most probably subsequent detachment of the cell from the extracellular matrix, occurs prior to cell death and that activation of a death pathway is subsequent to endothelial cell detachment, consistent with other findings (Rehn et al., 2001; Tarui et al., 2001). Many groups have suggested that vessel dissociation is a result of cell death, a consequence of withdrawal of growth factors (Jimenez et al., 2000). In our system, the removal of growth factors from the media did not cause a significant dissociation of HMEC-1 cords over a 36-hour period (supplementary material Fig. S5). This indicates that tropic factors play a role in vessel maturation but that

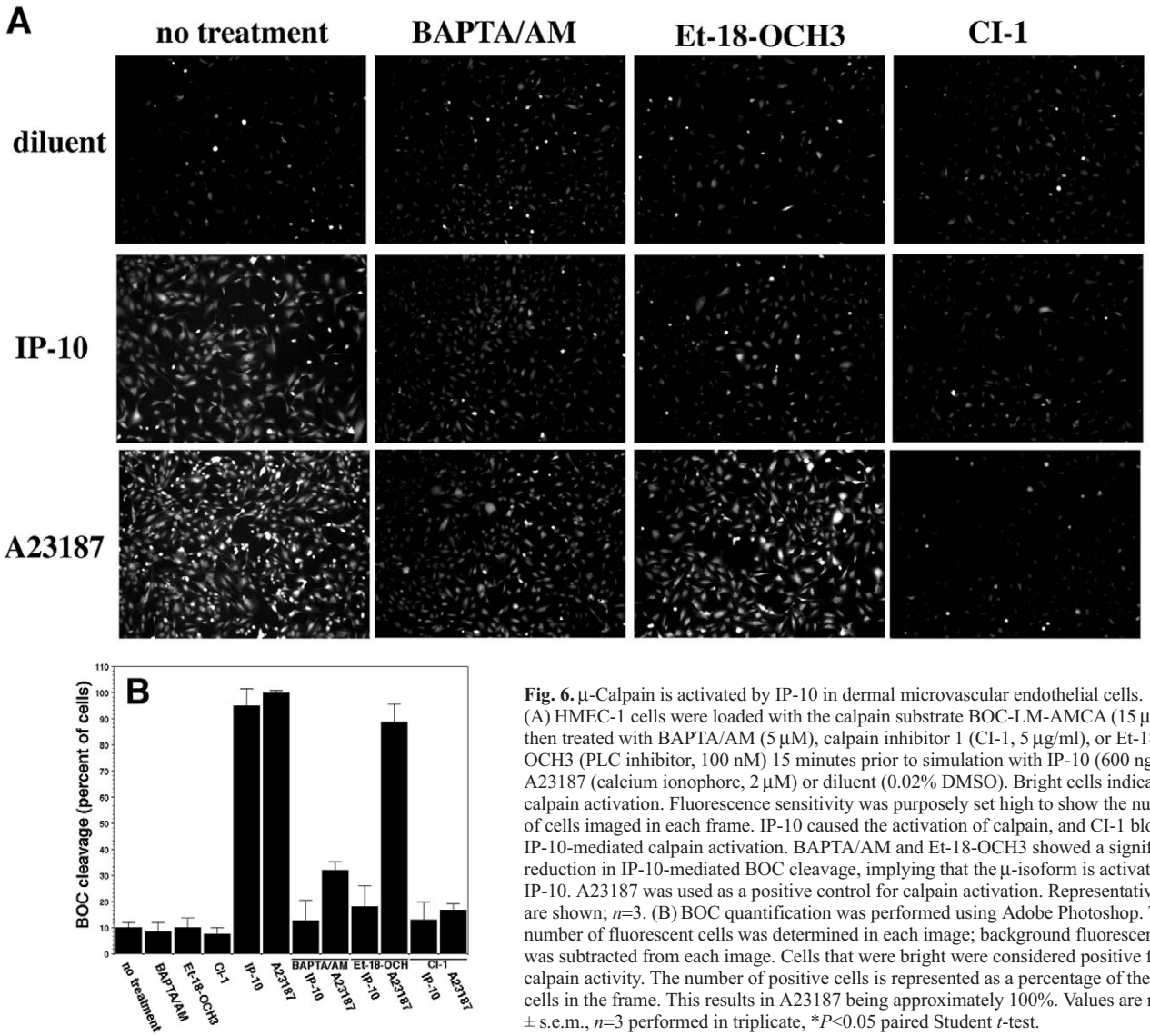

Fig. 6. μ-Calpain is activated by IP-10 in dermal microvascular endothelial cells. (A) HMEC-1 cells were loaded with the calpain substrate BOC-LM-AMCA (15 μM) then treated with BAPTA/AM (5 μM), calpain inhibitor 1 (CI-1, 5 μg/ml), or Et-18-OCH3 (PLC inhibitor, 100 nM) 15 minutes prior to simulation with IP-10 (600 ng/ml), A23187 (calcium ionophore, 2 μM) or diluent (0.02% DMSO). Bright cells indicated calpain activation. Fluorescence sensitivity was purposely set high to show the number of cells imaged in each frame. IP-10 caused the activation of calpain, and CI-1 blocked IP-10-mediated calpain activation. BAPTA/AM and Et-18-OCH3 showed a significant reduction in IP-10-mediated BOC cleavage, implying that the μ-isoform is activated by IP-10. A23187 was used as a positive control for calpain activation. Representative data are shown; n=3. (B) BOC quantification was performed using Adobe Photoshop. The number of fluorescent cells was determined in each image; background fluorescence was subtracted from each image. Cells that were bright were considered positive for calpain activity. The number of positive cells is represented as a percentage of the total cells in the frame. This results in A23187 being approximately 100%. Values are mean ± s.e.m., n=3 performed in triplicate, *P<0.05 paired Student t-test.

other mechanisms are involved in regulating vessel maturation and regression. To determine whether cell death is required for vessel dissociation, we pre-incubated endothelial cords with caspase inhibitors then treated with IP-10 or A23187 for 36 hours. Treatment with inhibitors of caspase 3 and caspase 9 did not inhibit cord dissociation (Fig. 10A,B). Camptothecin, a well-known activator of caspase 3 and inducer of apoptosis, was used as a positive control for cord dissociation via apoptosis; when pretreated with a caspase-3 inhibitor, camptothecin had no significant effect on endothelial cord dissociation (Fig. 10A,B). To determine whether cell death might occur through an alternate death pathway, we employed a TUNEL assay (Fig. 10C,D). Endothelial cords were pre-incubated with inhibitors to caspase 3 or CI-1 then treated with IP-10, A23187 or camptothecin for 36 hours. The cells were fixed and permeabilized, then stained with rhodamine-phalloidin (red, cell morphology) and TUNEL (green, apoptosis). Treatment with IP-10, A23187 and camptothecin alone presented cells positive for TUNEL staining (Fig. 10C). Again, when the endothelial cords were pretreated with an inhibitor of caspase 3 only a small number of cells were TUNEL positive, but cord dissociation occurred for IP-10 and A23187 but not for camptothecin (Fig. 10C). Treatment of the cords with CI-1 inhibited IP-10 or A23187 dissociation and significantly reduced TUNEL staining, whereas both dissociation and TUNEL staining occurred with the camptothecin treatment (Fig. 10C). In a similar experiment, the cells were treated with PI instead of rhodamine-phalloidin then analyzed for cell death (Fig. 8D). We found that pretreatment of the cords with CI-1 or a caspase-3 inhibitor significantly reduced the presence of TUNEL-positive cells for both IP-10 and A23187 treatment (Fig. 8D). In camptothecin-treated cords, pretreatment with CI-1 was unable to inhibit TUNEL staining, as observed with the caspase 3 inhibitor (Fig. 10D). These data provide substantial evidence that endothelial cord dissociation can occur in the absence of cell death and further provides evidence that IP-10-mediated vascular regression is most probably caused by the dissociation of endothelial cells from the extracellular matrix due to cleavage of integrin β3. Taken together, these data provide evidence to suggest that cell death results from the dissociation of focal adhesion complexes, which is mediated by calpain cleavage of β3 integrin, thus implying that cell death is downstream of β3 cleavage.

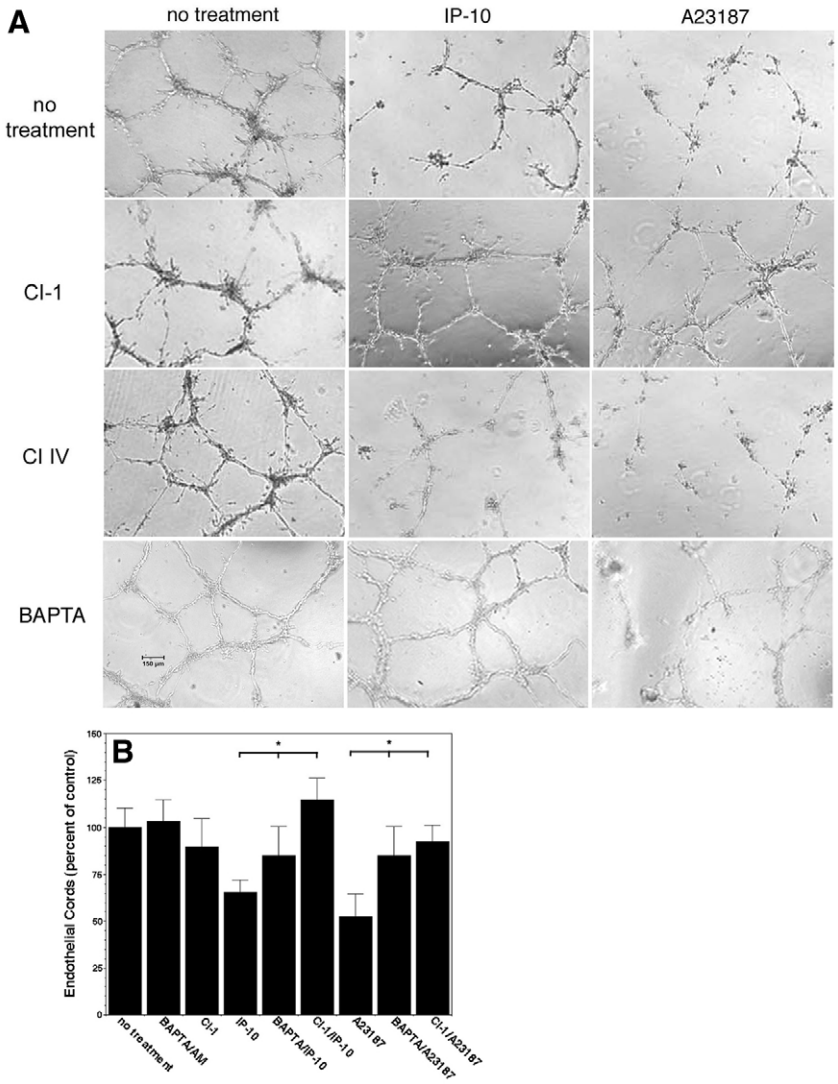

Fig. 7. Calpain activation is required for cord dissociation. (A) HMEC-1 cords were treated with CI-1 (5.0 μg/ml), CI IV (50 μM) and BAPTA/AM (2 μM) in 0.5% dialyzed FBS media for 30 minutes prior to treatment with IP-10 (600 ng/ml) and A23187 (2 μM) then further incubated for 24 hours. Both CI-1 and BAPTA/AM were able to inhibit cord dissociation but not CI IV, suggesting the involvement of μ-calpain. Scale bar: 150 μm. (B) Quantification of A shows a significant decrease in endothelial cords when treated with IP-10 or A23187. Pretreatment with BAPTA/AM or Et-18-OCH3 inhibited IP-10-mediated cord dissociation. Inhibition of IP-10 by the PLC inhibitor Et-18-OCH3 suggests that the PLC pathway is involved in μ-calpain activation. Endothelial cord area was determined using MetaMorph. The control (no treatment) was used as the base line and set at 100% with the other treatments set as a percentage. Values are mean ± s.e.m., n=3 performed in triplicate, *P<0.05 paired Student t-test.

Discussion

Angiogenesis is crucial during organogenesis and repair. While the mechanisms for the initiation of angiogenesis have been intensely investigated, those that limit and then reverse this have been less studied. As absence of this counter-regulation would lead to pathological vascularization, we have focused on signals that limit and then induce involution of new vessel growth. Earlier, we reported that CXCR3-binding chemokines, which appear late in wound healing, limit new vessel growth by inhibiting endothelial cell migration (Bodnar et al., 2006). However, this is only half the equation; during wound resolution the exuberant vascular tree regresses to a relatively avascular dermis. Herein, we show that these same chemokines can also induce vessel regression. However, this second crucial step is accomplished by divergent downstream signals. For vessel regression, activation of CXCR3 by ligand binding triggers μ-calpain, which cleaves the tail of the β3 integrin, leading to endothelial cell dissociation and cell death.

CXCR3 is a seven transmembrane G-protein-coupled receptor that, via 5′ splicing, exists as an A or B isomer. These CXCR3 isomers can trigger diverse downstream pathways dependent on the linked heterotrimeric G protein. The A-isomer has been shown to induce migration and proliferation, and the B-isomer to inhibit migration and proliferation (Lasagni et al., 2003). In fibroblasts, this receptor actuates the cAMP-PKA pathway, which results in negative phosphorylation of m-calpain to prevent growth-factor-induced motility (Shiraha et al., 2002). In keratinocytes, CXCR3 is linked to activation of PLCβ to induce a calcium-flux-mediated activation of μ-calpain enabling greater motility (Satish et al., 2005). Whereas we found earlier that endothelial cells utilized the cAMP-PKA pathway to inhibit m-calpain (Bodnar et al., 2006), we now report that the PLC-calcium flux pathway is also present in these cells and leads to μ-calpain activation. Here, we provide evidence that the active μ-calpain clips the tail of the β3 integrin, leading to endothelial cell dissociation and anoikis. This mechanism by which CXCR3 signaling may cause endothelial dissociation and death has also been noted in platelets (Xi et al., 2006). Thus, the same CXCR3 not only limits new vessel growth but also induces vascular involution, demonstrating parsimony of signaling network functionality. Further, this study shows that the ELR-negative chemokines may have a greater affect on specific vascular structures. We found that IP-10 (CXCL10) and PF4 (CXCL4) were able to destabilize vessels and tubes of microvascular origin (Figs 2, 3 and 4), which were found to readily express CXCR3 (Fig. 4B; supplementary material Figs S2 and

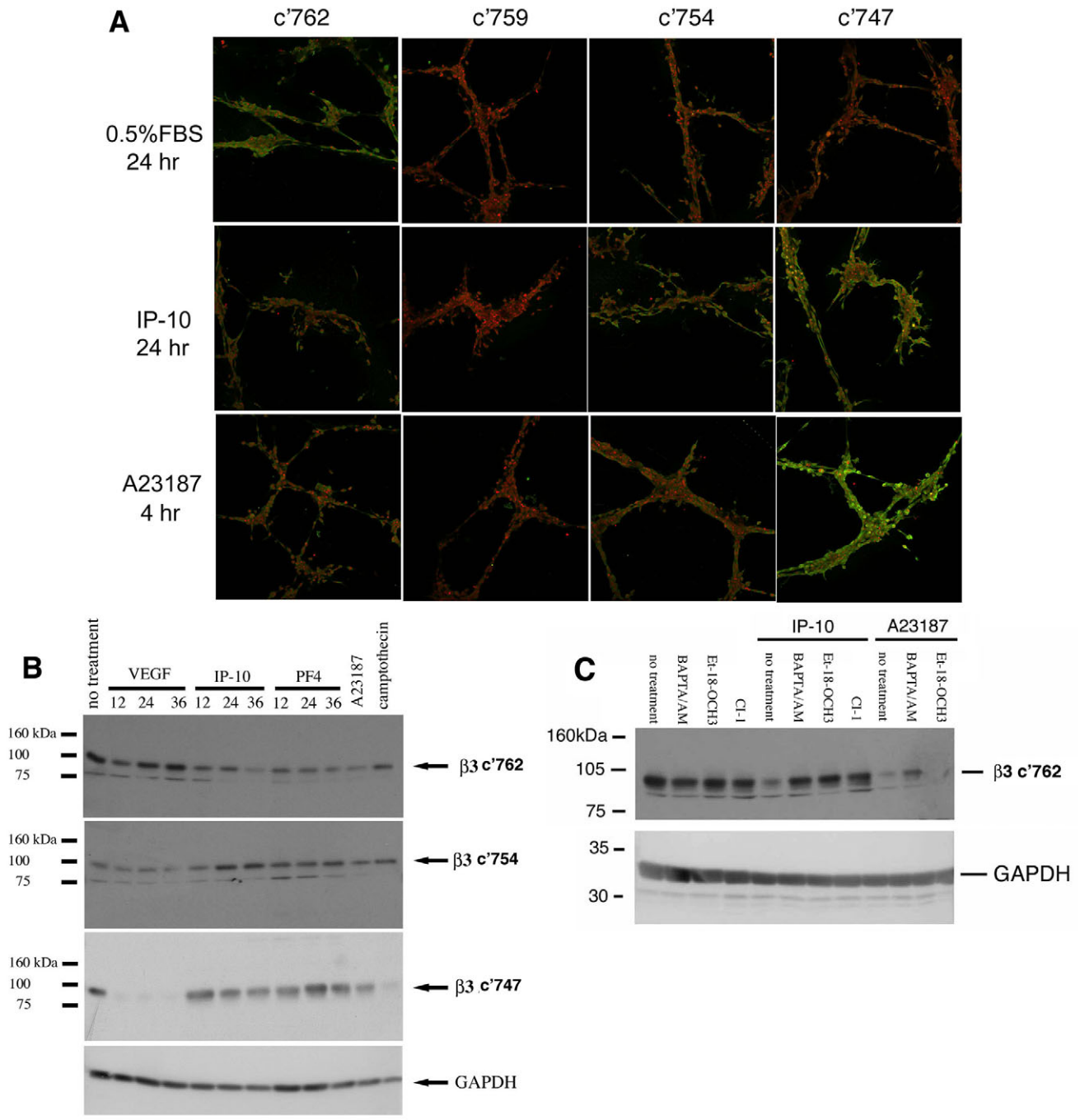

Fig. 8. IP-10 causes cleavage of β3 integrin. (A) HMEC-1 cords were incubated with IP-10 (600 ng/ml) or A23187 (2 μM). The cords were fixed, permeabilized then stained for cleavage of β3 integrin using an antibody that recognizes β3 integrin (c'762, full length) and specific calpain cleavage sites c'754 and c'747 (Xi et al., 2003) (green) and PI (nuclear stain, red). These data indicate that IP-10 causes the cleavage of β3 integrin at the calpain cleavage site c'754 and c'747, as indicated by green staining. (B) HMEC-1 cells were grown on plastic then treated with VEGF-A (75 ng/ml), IP-10 (600 ng/ml), PF4 (400 ng/ml) or A23187 (2 μM) for various times. To analyze β3 cleavage, antibodies recognizing the C-terminal five amino acids of β3 integrin, c'762 (full length) and specific calpain cleavage sites c'754, and c'747 (Xi et al., 2003) were used. A decrease in staining of the full-length antibody (c'762) indicates cleavage of β3 integrin. Staining with the antibodies that recognize c'754 or c'747 indicates cleavage at these specific μ-calpain sites. (C) HMEC-1 grown on plastic were treated with BAPTA/AM (5 μM), calpain inhibitor 1 (CI-1, 5 mM), or Et-18-OCH3 (100 nM) prior to stimulation with IP-10 (600 ng/ml) or A23187 (2 μM). After 24 hours the cells were lysed and analyzed for β3 cleavage. A decrease in c'762 staining indicates cleavage of the cytoplasmic domain of β3 integrin. BAPTA/AM and Et-18-OCH3 are able to inhibited cleavage of β3 integrin by IP-10 (increased staining). These data indicate that cleavage is due to calpain activation. Shown is one experiment of three.

S4), but did not have an effect on HUVEC (Fig. 4A), which were shown to have very low-to-no expression of CXCR3 (Fig. 4B; supplementary material Fig. S4). Although Mig (CXCL9) and IP-9 (CXCL11) are ligands for CXCR3, we did not look at their ability to induce regression due to their lower affinity for CXCR3-B, which has been shown to be the only CXCR3 isoform expressed on these endothelial cells (Lasagni et al., 2003). We also note that HMEC-1 cells did not form vascular structures (tubes) in collagen

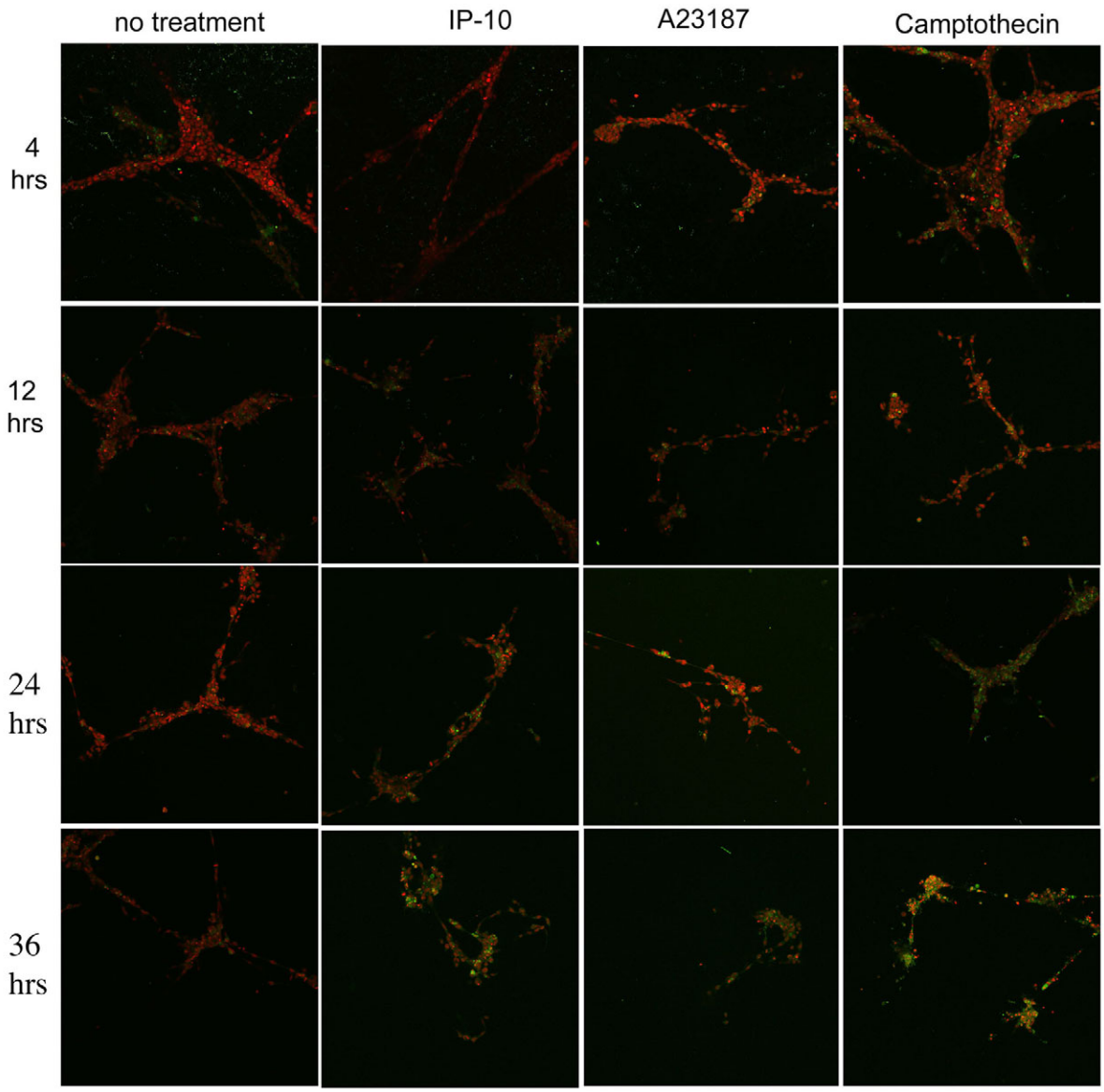

Fig. 9. IP-10 causes endothelial cell death. HMEC-1 cords were treated with IP-10 (600 ng/ml), A23187 (2 μM) or Camptothecin (3 μM) from 4 to 36 hours. The cells were fixed, permeabilized and immunostained using fluorescence antibodies against activated caspase 3 (green). Nuclei were stained with PI (red). Significant caspase activation was observed with IP-10 treatment after 24 hours when cord dissociation has already occurred. Representative data from three experiments are shown.

as readily as HUVEC (data not shown), consistent with the literature of tube formation being tested on collagen for HUVEC but in Matrigel for microvascular endothelial cells. These results demonstrate inherent differences between endothelial cells, suggesting that multiple signaling networks modulate vascular involution and remodeling.

Not unsurprisingly, the ligand with low affinity for CXCR3B, IP-9, did not drive involution (supplementary material Fig. S3). As IP-9 does not bind well to CXCR3B, this probably is simply due to failure to activate CXCR3 downstream signaling. This failure to drive CXCR3 from IP-9 is not needed because IP-10 is the main ligand in the dermis during the remodeling phase of wound repair (Yates et al., 2007). Thus, the vasculature would be 'pruned' at its base. The functioning of PF4 is more speculative. This ligand is released at high levels during the initial platelet activation and degranulation. This would place the ligand at the right time to destabilize the vessels to set the stage for exuberant angiogenesis during the regenerative phase. It also is possible that PF4 prevents premature angiogenesis prior to the establishment of a stable platelet plug.

The varied levels of CXCR3 expression on endothelial cells suggest that the ELR-negative chemokines are only one mechanism whereby the vascular tree is pruned. In wounds in mice lacking CXCR3, the initially exuberant vascular tree does involute, though at a slower rate (Yates et al., 2007) (Fig. 2B), implicating a redundancy of this important function. This may be accomplished by loss of trophic factors or other active signals for involution. A small number of pro-involution factors have been proposed, the major ones being Ang2, angiostatin, endostatin and extracellular proteases (Davis and Saunders, 2006; Nyberg et al., 2005; Tait and

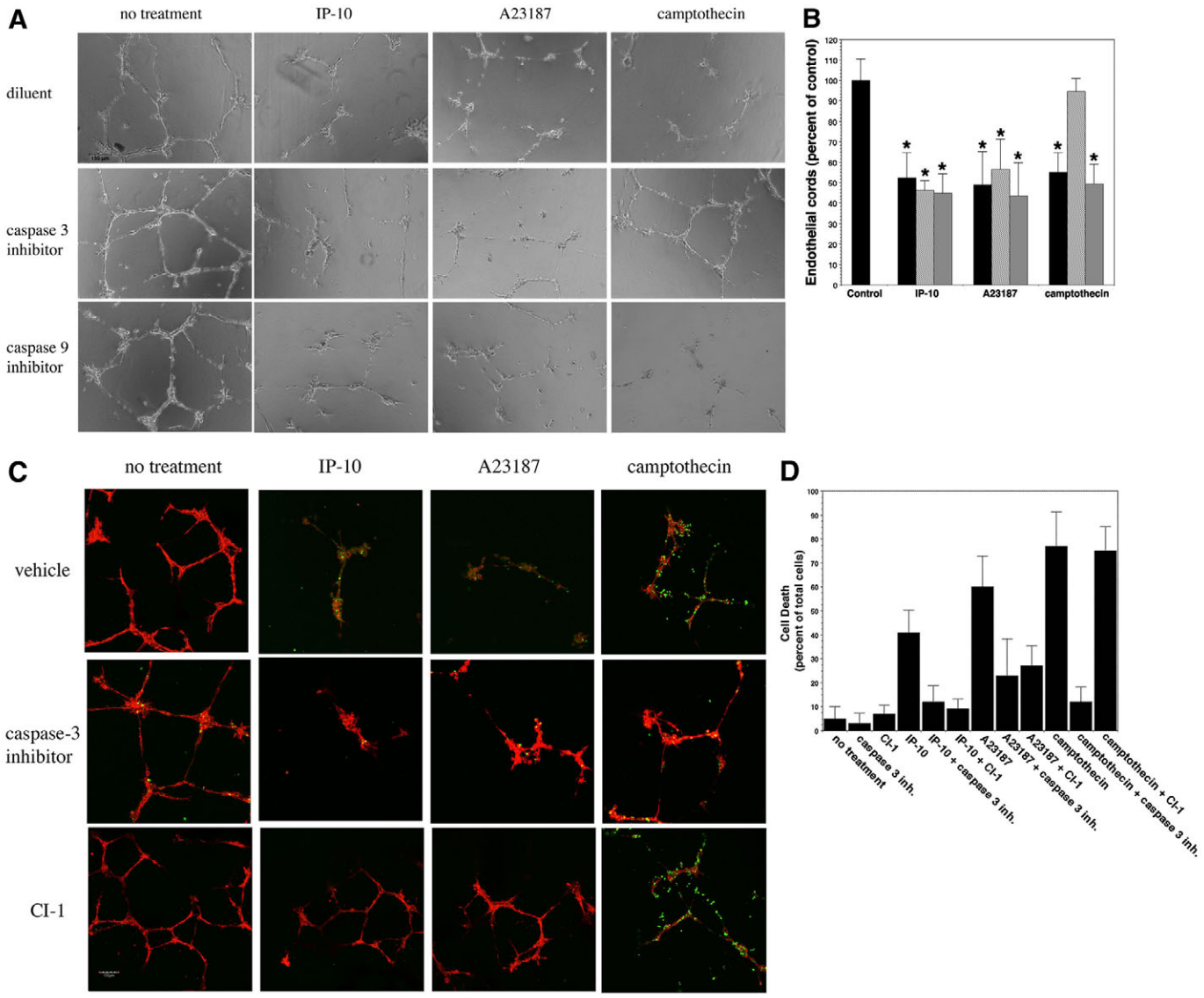

Fig. 10. Caspase blockade prevents cell death but not vessel dissociation. (A) HMEC-1 cords were treated with CI-1 (5 μM), caspase 3 (Z-VDVAD-FMK, 3 μM) and caspase 9 (Z-LEHD-FMK, 3 μM) inhibitors prior to stimulation with IP-10 (600 ng/ml), A23187 (2 μM) or camptothecin (3 μM) then further incubated for 36 hours. Pretreatment of cords with the caspase inhibitors did not reverse the dissociation effects of IP-10, whereas dissociation was not observed in the camptothecin-treated cords when the caspase inhibitors were added. The figures are representative of four experiments. Scale bar: 150 μm. (B) Quantification of A shows that inhibition of caspase 3 or caspase 9 did not inhibit IP-10-mediated dissociation. Pretreatment of camptothecin with a caspase 3 inhibitor significantly inhibited endothelial cord dissociation. These data suggest that IP-10-induced endothelial cord dissociation is upstream of caspase 3 activation. Endothelial cord area was determined using MetaMorph. The control (no treatment) was used as the base line and set at 100% with the other treatments set as a percentage. Black bars, no treatment; hatched bars, treatment with caspase 3 inhibitor; gray bars, treatment with caspase 9 inhibitor. Values are mean ± s.e.m., n=3 performed in triplicate, *P<0.05 paired Student t-test. (C) For the TUNEL assay, cells were treated as stated in A with the addition of CI-1 (5 μM). The cords were fixed and permeabilized, then analyzed for apoptosis (green). Cells were counterstained with rhodamine-phalloidin (red) for cell morphology. Cords incubated with IP-10 (600 ng/ml), A23187 (2 μM) or camptothecin (3 μM, positive control) demonstrated significant TUNEL staining compared to untreated cords (diluent). When the cells were pretreated with the caspase 3 inhibitor, TUNEL staining was significantly decreased. Note that there is still significant cord regression in the IP-10-treated cords and that CI-1 showed a significant inhibition of both dissociation and apoptosis. The figures are representative of triplicate experiments. Scale bar: 150 μm. (D) Endothelial cords treated as stated in C were fixed and permeabilized, then analyzed for apoptosis using the TUNEL assay. The cells were counterstained with PI (nuclei). The number of TUNEL-positive cells for each treatment is indicated as a percentage of total cells. The results are an average of triplicate experiments.

Jones, 2004). However, these other factors have yet to be placed at the time of vessel regression upon successful skin wound repair. Still, it is not unexpected that the critical vascular regression event is controlled by redundant signals.

This leaves open the question of whether one needs downregulation of pro-angiogenic factors to achieve involution. We find that CXCR3 signaling is dominant over VEGF in vitro and in vivo for both inhibition of angiogenesis (Bodnar et al., 2006) and regression (Figs 2-4). Other pro-involution factors such as proteases also appear to act dominantly (Davis and Saunders, 2006). These findings might imply that vascular regression results simply from turning on a negative attenuator. However, the requirement of VEGF

for the maintenance and/or maturation of vessels is not well established. There are some in vivo correlative studies that demonstrate diminution of angiogenic factors such as VEGF concurrent with vascular involution (Benjamin et al., 1999). However, a recent study suggests that VEGF is a negative regulator of vessel maturation (Greenberg et al., 2008). Also, association of αvβ3 integrin with VEGFR-2 is necessary for VEGFR-2 activation (Mahabeleshwar et al., 2007), suggesting that cleavage of β3 integrin may limit VEGFR-2 function. There is also a VE-cadherin-VEGFR-2 association that has been shown to play a role in cell survival (Carmeliet et al., 1999). Disruption of the VEGFR-2 stabilization by degradation of β3 integrin may play a role in vessel dissociation by tipping the balance towards apoptosis from survival. This dual regulatory control could allow for finer rheostatting of the response. In addition, it could enable differential signaling of the same factor to two different cell types. One example of this could be for TGFβ to drive collagen production from fibroblasts, even while the vascular tree involutes under the influence of CXCR3 chemokines or other signals; this situation is present during scar formation (Brunner and Blakytny, 2004). These findings impel us to consider that even 'disuse atrophy' involves not only loss of trophic factors but also the emergence of active atrophic factors.

We have focused on calpain cleavage of the cytoskeleton-interacting and regulatory tail of the β3 integrin as the molecular mechanism underlying CXCR3-induced vessel involution. This is because the β3 integrin is the major β-subunit functioning in endothelial cells. However, the target NPLY motif is not limited to β3 integrin. This motif is also found in β1 integrin (two motifs), β2 integrin (two NPXF motifs), β5 integrin (two motifs), β6 integrin (two motifs) and β7 integrin (one NPLY and one NPXF motif) leading to the possibility that calpain cleavage of integrin in endothelial cells may not be limited to just the β3 integrin.

The data presented herein pose the possible use of agonists that specifically target CXCR3B as potential therapies for pathological angiogenesis. It is well established that IP-10 and PF4 are inhibitors of tumor angiogenesis (Giese et al., 2002; Lazzeri and Romagnani, 2005; Yamaguchi et al., 2005); therefore specific activation of CXCR3B might provide a greater anti-angiogenic effect. However, CXCR3B activation might also lead to pathological vessel involution. In acute graft-versus-host disease, CXCR3 and IP-10 have been shown to play a significant role in the pathogenesis of tissue rejection (Piper et al., 2007). The neutralization of either IP-10 or CXCR3 function, similar to Avastin blockade of VEGF signaling, could be utilized as a possible adjunct for improved graft survival and might provide an enhancement in vessel growth to aid in the repair of inflammatory pathological conditions such as ulcers.

A number of questions remain open. First and foremost is how some vasculature are maintained despite the CXCR3 ligand-rich environment and loss of trophic factors. This may happen at two levels – loss of sensitivity to these ligands or intracellular resistance. There is precedence for the latter as β3 integrin in platelets is phosphorylated upon thrombin activation, making this integrin significantly less susceptible to μ-calpain cleavage than to A23187 treatment (Xi et al., 2006). The other mechanism may involve CXCR3 downregulation in mature vessels or in those maintained by active blood flow (Fig. 1B) (Burdick et al., 2005). Both need to be explored in further studies. Lastly, the role of accessory cells such as pericytes in being trophic for vascular maintenance or contributory to involution remains to be investigated.

Materials and Methods

All studies with human cells were deemed exempt by the University of Pittsburgh IRB and Pittsburgh VA Medical Center; all animal studies were approved by the animal care committees of both these institutions.

Cell culture

Human dermal microvascular endothelial cells (HMEC-1) (Ades et al., 1992) were obtained from the CDC (Atlanta, Georgia). Adult dermal microvascular (dHMEC), human lung microvascular (hLMEC) and human umbilical vein endothelial cells (HUVEC) were purchased from Lonza (Allendale, NJ).

In vitro Matrigel assay

In vitro cord dissociation was assessed using a modification of a previously reported method (Bodnar et al., 2006). To form the cords, HMEC-1 (Ades et al., 1992) were plated on Matrigel in 2.5% FBS-MCDB131 with 75 ng/ml VEGF or 50 ng/ml bFGF. After 24 hours the media was removed and replaced with 0.5% dialyzed FBS-MCDB131 with VEGF (75 ng/ml), bFGF (50 ng/ml), IP-10 (600 ng/ml), PF4 (400 ng/ml), IL-8 (100 ng/ml), A-23187 (2 μM), calpain inhibitor I (ALLN/CI-1, 5 μM), calpain inhibitor IV (CI IV, 25 μM), BAPTA/AM (2 μM), caspase 3 (Z-DEVD-FMK) and caspase 9 (Z-LEHD-FMK) inhibitors (3 μM), or camptothecin (4 μM), and incubated as indicated in the figure legends. A dose-response curve was used to determine the concentration of IP-10 (supplementary material Fig. S1).

For the neutralization antibody experiments, cords were allowed to form as stated above. IP-10 neutralizing antibody (25 ng, R&D Bioscience) was incubated with IP-10 in 0.5% dialyzed FBS-MCDB131 media 30 minutes prior to addition to formed cords. For the CXCR3, neutralizing antibody (0.5 ng, R&D Bioscience) was added to the formed cords 30 minutes prior to the addition of IP-10, incubated for 24 hours and then imaged.

Quantification of the tubes was performed by taking three 4× images (non-overlapping) of each chamber, then the cord density for each image was analyzed by MetaMorph and averaged together. The average of at least three chambers was used to determine cord density for each treatment. The average cord density is represented as a percentage of the untreated control.

In vivo Matrigel plug assay

In vivo vessel regression was tested using a modification of a previously reported method (Bodnar et al., 2006). Matrigel with VEGF was injected subcutaneously into the ventral side of C57B1/6 female mice in the groin area near the dorsal midline. Two injections were made, one on the left and one on the right side. On days 10 and 12, one side was injected with 5 μg of IP-10; the opposite side (control) was injected with an equal volume of saline in the area of the initial Matrigel injection. On day 17, the Matrigel was removed and paraffin embedded. The Matrigel plugs were analyzed for vessels by Masson's trichrome and vWF staining. A total of 13 mice were used, three for day 10 and 10 for saline and IP-10 treatments.

Wounding assay

CXCR3 Knockout (*CXCR3*$^{-/-}$) mice were engineered as previously described (Hancock et al., 2000). *CXCR3*$^{-/-}$ female mice were bred with *CXCR3*$^{-/-}$ male and all offspring were genotyped before use. Male and female mice 7-8 weeks of age and weighing approximately 25 g were wounded as previously described (Yates et al., 2007). Mouse wound bed biopsies surrounded by a margin of non-wounded skin were collected at days 14 and 30 post-wounding. Tissue sections were H&E stained and stained for vWF. Biopsies were also stained for vWF (Abcam) and CXCR3 (R&D Bioscience) and visualized with a secondary antibody conjugated with Texas red or FITC, respectively.

Qualitative assessments of vascularization of the wound tissue were performed by a trained pathologist by quantifying the number of capillaries as determined by vWF staining and morphometry, using a 10× objective lens along the wound surface. Three to four images spanning the length of the wounded tissue having minimal overlap were acquired for each wound. The average number of vessels per 10× field was determined for each wound. The number of vessels observed within the wound tissue was determined from three independent experiments with six mice for each time point.

Calpain assay

In vitro calpain activity assay was carried out by using the membrane permeable substrate BOC as described previously (Glading et al., 2004). In brief, HMEC-1 cells were grown on gelatin-coated slides then incubated in serum-reduced media. The cells were treated with BAPTA/AM (5 μM), Et-18-OCH3 (100 nM) or CI-1 (5 μM) prior to the addition of BOC (15 μM). The cells were further incubated with IP-10 (200 ng/ml), A23187 (2 μM) or an equal volume of diluent as indicated by the figure. The cleavage of BOC by calpain was visualized using a fluorescence microscope and images were captured using a SPOT Flex camera. Quantification of positive cells was performed by counting the total number of cells and the fluorescent cells in a 10× images using MetaMorph. The individual fluorescence was determined in each image; background fluorescence was calculated using the negative control and subtracted for each image. Cells that were bright were considered positive for calpain activity. The average of three images for each well was determined and a minimum

of three wells was used to determine calpain activity for each treatment. The number of positive cells is represented as a percentage of the total number of cells in the frame.

Immunoblotting

HMEC-1 (60-70% confluent) were incubated with 0.5% dialyzed FBS-MCDB131 with various compounds and incubated as indicated in the figure legend. The cells were lysed then immunoblotted for cleavage of β3 integrin using site-specific antibodies that only recognize the C-terminal domain of β3 integrin when it is cleaved C-terminal to the amino acid residues Y759 (c'759), F754 (c'754) and Y747 (c'747), and the full-length β3 cytoplasmic domain recognizes the C-terminal five amino acids (c'762) (Xi et al., 2003). These residues are based on the amino acid sequence of the human β3 integrin (accession number: P05106). Protein staining was visualized using ECL.

Immunofluorescence

Endothelial cords were formed as stated above. The formed cords were treated with IP-10, A23187 or camptothecin for a varying amount of time, then fixed, permeabilized and analyzed for cleavage of β3 integrin. The cells were stained with antibody against the cytoplasmic tail of β3 integrin that recognizes known μ-calpain cleavage sites (Xi et al., 2003) and visualized. Cell death was analyzed by immunostaining the cords with an active caspase-3-specific antibody and the TUNEL assay. In the TUNEL analysis, cells were counterstained with rhodamine-phalloidin or PI. Cells were imaged using the Olympus fluoview FV1000 confocal microscope. Quantification of TUNEL staining was performed by determining the percentage of TUNEL-positive cells in the total number of cells. PI was used to identify individual cells.

Data analysis

For quantification of cords, images were quantitatively analyzed using MetaMorph version 7.0, as previously described (Yates et al., 2007). In brief, tubes were segmented to exclude background from analysis and the percent area of the endothelial cords or tubes was measured. Each data point is an average of cord area from three 4× images of each sample performed in triplicate. For quantification of calpain activity, the number of BOC-positive cells was determined by removing the background averaged fluorescence (determined by the control, no treatment); fluorescent cells were considered positive and were represented as a percentage of the total number of cells. Each data point is an average of three 10× images from three separate experiments. Analysis was performed using Photoshop 7.0. The integrated morphometry analysis in MetaMorph was used to analyze TUNEL staining. MetaMorph was used to count positive and total cell numbers. These values are represented as a percentage of total cells. The number of TUNEL-positive cells was averaged and represented as a percentage of the total number of cells. All experiments were performed at least three times, each in triplicate. Statistical significance was determined using the Student *t*-test (paired) with significance assigned for $P<0.05$.

We would like to thank Diana Whaley for technical support and the members of the Wells laboratory for helpful comments. This study was supported by funds from VA Medical Research Program and National Institute of General Medical Sciences (NIH). The authors have no conflicts of interests to disclosure. Deposited in PMC for release after 12 months.

References

Ades, E. W., Candal, F. J., Swerlick, R. A., George, V. G., Summers, S., Bosse, D. C. and Lawley, T. J. (1992). HMEC-1: establishment of an immortalized human microvascular endothelial cell line. *J. Invest. Dermatol.* **99**, 683-690.

Benjamin, L. E., Golijanin, D., Itin, A., Pode, D. and Keshet, E. (1999). Selective ablation of immature blood vessels in established human tumors follows vascular endothelial growth factor withdrawal. *J. Clin. Invest.* **103**, 159-165.

Bodnar, R. J., Yates, C. C. and Wells, A. (2006). IP-10 blocks vascular endothelial growth factor-induced endothelial cell motility and tube formation via inhibition of calpain. *Circ. Res.* **98**, 617-625.

Booth, V., Keizer, D. W., Kamphuis, M. B., Clark-Lewis, I. and Sykes, B. D. (2002). The CXCR3 binding chemokine IP-10/CXCL10: structure and receptor interactions. *Biochemistry* **41**, 10418-10425.

Brunner, G. and Blakytny, R. (2004). Extracellular regulation of TGF-beta activity in wound repair: growth factor latency as a sensor mechanism for injury. *Thromb. Haemost.* **92**, 253-261.

Burdick, M. D., Murray, L. A., Keane, M. P., Xue, Y. Y., Zisman, D. A., Belperio, J. A. and Strieter, R. M. (2005). CXCL11 attenuates bleomycin-induced pulmonary fibrosis via inhibition of vascular remodeling. *Am. J. Respir. Crit. Care Med.* **171**, 261-268.

Carmeliet, P., Lampugnani, M. G., Moons, L., Breviario, F., Compernolle, V., Bono, F., Balconi, G., Spagnuolo, R., Oosthuyse, B., Dewerchin, M. et al. (1999). Targeted deficiency or cytosolic truncation of the VE-cadherin gene in mice impairs VEGF-mediated endothelial survival and angiogenesis. *Cell* **98**, 147-157.

Davis, G. E. and Saunders, W. B. (2006). Molecular balance of capillary tube formation versus regression in wound repair: role of matrix metalloproteinases and their inhibitors. *J. Invest. Dermatol. Symp. Proc.* **11**, 44-56.

Feldman, E. D., Weinreich, D. M., Carroll, N. M., Burness, M. L., Feldman, A. L., Turner, E., Xu, H. and Alexander, H. R., Jr (2006). Interferon gamma-inducible protein 10 selectively inhibits proliferation and induces apoptosis in endothelial cells. *Ann. Surg. Oncol.* **13**, 125-133.

Flevaris, P., Stojanovic, A., Gong, H., Chishti, A., Welch, E. and Du, X. (2007). A molecular switch that controls cell spreading and retraction. *J. Cell Biol.* **179**, 553-565.

Giese, N. A., Raykov, Z., DeMartino, L., Vecchi, A., Sozzani, S., Dinsart, C., Cornelis, J. J. and Rommelaere, J. (2002). Suppression of metastatic hemangiosarcoma by a parvovirus MVMp vector transducing the IP-10 chemokine into immunocompetent mice. *Cancer Gene Ther.* **9**, 432-442.

Glading, A., Bodnar, R. J., Reynolds, I. J., Shiraha, H., Satish, L., Potter, D. A., Blair, H. C. and Wells, A. (2004). Epidermal growth factor activates m-calpain (calpain II), at least in part, by extracellular signal-regulated kinase-mediated phosphorylation. *Mol. Cell. Biol.* **24**, 2499-2512.

Greenberg, J. I., Shields, D. J., Barillas, S. G., Acevedo, L. M., Murphy, E., Huang, J., Scheppke, L., Stockmann, C., Johnson, R. S., Angle, N. et al. (2008). A role for VEGF as a negative regulator of pericyte function and vessel maturation. *Nature* **456**, 809-813.

Hancock, W. W., Lu, B., Gao, W., Csizmadia, V., Faia, K., King, J. A., Smiley, S. T., Ling, M., Gerard, N. P. and Gerard, C. (2000). Requirement of the chemokine receptor CXCR3 for acute allograft rejection. *J. Exp. Med.* **192**, 1515-1520.

Jimenez, B., Volpert, O. V., Crawford, S. E., Febbraio, M., Silverstein, R. L. and Bouck, N. (2000). Signals leading to apoptosis-dependent inhibition of neovascularization by thrombospondin-1. *Nat. Med.* **6**, 41-48.

Kouroumalis, A., Nibbs, R. J., Aptel, H., Wright, K. L., Kolios, G. and Ward, S. G. (2005). The chemokines CXCL9, CXCL10, and CXCL11 differentially stimulate G alpha i-independent signaling and actin responses in human intestinal myofibroblasts. *J. Immunol.* **175**, 5403-5411.

Lasagni, L., Francalanci, M., Annunziato, F., Lazzeri, E., Giannini, S., Cosmi, L., Sagrinati, C., Mazzinghi, B., Orlando, C., Maggi, E. et al. (2003). An alternatively spliced variant of CXCR3 mediates the inhibition of endothelial cell growth induced by IP-10, Mig, and I-TAC, and acts as functional receptor for platelet factor 4. *J. Exp. Med.* **197**, 1537-1549.

Lazzeri, E. and Romagnani, P. (2005). CXCR3-binding chemokines: novel multifunctional therapeutic targets. *Curr. Drug Targets Immune Endocr. Metabol. Disord.* **5**, 109-118.

Lobov, I. B., Rao, S., Carroll, T. J., Vallance, J. E., Ito, M., Ondr, J. K., Kurup, S., Glass, D. A., Patel, M. S., Shu, W. et al. (2005). WNT7b mediates macrophage-induced programmed cell death in patterning of the vasculature. *Nature* **437**, 417-421.

Mahabeleshwar, G. H., Feng, W., Reddy, K., Plow, E. F. and Byzova, T. V. (2007). Mechanisms of integrin-vascular endothelial growth factor receptor cross-activation in angiogenesis. *Circ. Res.* **101**, 570-580.

Meredith, J., Jr, Mu, Z., Saido, T. and Du, X. (1998). Cleavage of the cytoplasmic domain of the integrin beta3 subunit during endothelial cell apoptosis. *J. Biol. Chem.* **273**, 19525-19531.

Nyberg, P., Xie, L. and Kalluri, R. (2005). Endogenous inhibitors of angiogenesis. *Cancer Res.* **65**, 3967-3979.

Perrin, B. J. and Huttenlocher, A. (2002). Calpain. *Int. J. Biochem. Cell Biol.* **34**, 722-725.

Piper, K. P., Horlock, C., Curnow, S. J., Arrazi, J., Nicholls, S., Mahendra, P., Craddock, C. and Moss, P. A. (2007). CXCL10-CXCR3 interactions play an important role in the pathogenesis of acute graft-versus-hist disease in the skin following allogeneic stem-cell transplantation, *Blood* **110**, 3827-3832.

Rehn, M., Veikkola, T., Kukk-Valdre, E., Nakamura, H., Ilmonen, M., Lombardo, C., Pihlajaniemi, T., Alitalo, K. and Vuori, K. (2001). Interaction of endostatin with integrins implicated in angiogenesis. *Proc. Natl. Acad. Sci. USA* **98**, 1024-1029.

Romagnani, P., Annunziato, F., Lasagni, L., Lazzeri, E., Beltrame, C., Francalanci, M., Uguccioni, M., Galli, G., Cosmi, L., Maurenzig, L. et al. (2001). Cell cycle-dependent expression of CXC chemokine receptor 3 by endothelial cells mediates angiostatic activity. *J. Clin. Invest.* **107**, 53-63.

Salcedo, R., Resau, J. H., Halverson, D., Hudson, E. A., Dambach, M., Powell, D., Wasserman, K. and Oppenheim, J. J. (2000). Differential expression and responsiveness of chemokine receptors (CXCR1-3) by human microvascular endothelial cells and umbilical vein endothelial cells. *FASEB J.* **14**, 2055-2064.

Satish, L., Blair, H. C., Glading, A. and Wells, A. (2005). Interferon-inducible protein 9 (CXCL11)-induced cell motility in keratinocytes requires calcium flux-dependent activation of mu-calpain. *Mol. Cell. Biol.* **25**, 1922-1941.

Shiraha, H., Glading, A., Chou, J., Jia, Z. and Wells, A. (2002). Activation of m-calpain (calpain II) by epidermal growth factor is limited by protein kinase A phosphorylation of m-calpain. *Mol. Cell. Biol.* **22**, 2716-2727.

Struyf, S., Burdick, M. D., Peeters, E., Van den Broeck, K., Dillen, C., Proost, P., Van Damme, J. and Strieter, R. M. (2007). Platelet factor-4 variant chemokine CXCL4L1 inhibits melanoma and lung carcinoma growth and metastasis by preventing angiogenesis. *Cancer Res.* **67**, 5940-5948.

Tait, C. R. and Jones, P. F. (2004). Angiopoietins in tumours: the angiogenic switch. *J. Pathol.* **204**, 1-10.

Tarui, T., Miles, L. A. and Takada, Y. (2001). Specific interaction of angiostatin with integrin alpha(v)beta(3) in endothelial cells. *J. Biol. Chem.* **276**, 39562-39568.

Tsubaki, T., Takegawa, S., Hanamoto, H., Arita, N., Kamogawa, J., Yamamoto, H., Takubo, N., Nakata, S., Yamada, K., Yamamoto, S. et al. (2005). Accumulation of

plasma cells expressing CXCR3 in the synovial sublining regions of early rheumatoid arthritis in association with production of Mig/CXCL9 by synovial fibroblasts. *Clin. Exp. Immunol.* **141**, 363-371.

Xi, X., Bodnar, R. J., Li, Z., Lam, S. C. and Du, X. (2003). Critical roles for the COOH-terminal NITY and RGT sequences of the integrin beta3 cytoplasmic domain in inside-out and outside-in signaling. *J. Cell Biol.* **162**, 329-339.

Xi, X., Flevaris, P., Stojanovic, A., Chishti, A., Phillips, D. R., Lam, S. C. and Du, X. (2006). Tyrosine phosphorylation of the integrin beta 3 subunit regulates beta 3 cleavage by calpain. *J. Biol. Chem.* **281**, 29426-29430.

Yamaguchi, K., Ogawa, K., Katsube, T., Shimao, K., Konno, S., Shimakawa, T., Yoshimatsu, K., Naritaka, Y., Yagawa, H. and Hirose, K. (2005). Platelet factor 4 gene transfection into tumor cells inhibits angiogenesis, tumor growth and metastasis. *Anticancer Res.* **25**, 847-851.

Yang, J. and Richmond, A. (2004). The angiostatic activity of interferon-inducible protein-10/CXCL10 in human melanoma depends on binding to CXCR3 but not to glycosaminoglycan. *Mol. Ther.* **9**, 846-855.

Yao, L., Pike, S. E., Pittaluga, S., Cherney, B., Gupta, G., Jaffe, E. S. and Tosato, G. (2002). Anti-tumor activities of the angiogenesis inhibitors interferon-inducible protein-10 and the calreticulin fragment vasostatin. *Cancer Immunol. Immunother.* **51**, 358-366.

Yates, C. C., Whaley, D., Kulasekeran, P., Hancock, W. W., Lu, B., Bodnar, R., Newsome, J., Hebda, P. A. and Wells, A. (2007). Delayed and deficient dermal maturation in mice lacking the CXCR3 ELR-negative CXC chemokine receptor. *Am. J. Pathol.* **171**, 484-495.

Yates, C. C., Whaley, D., Y-Chen, A., Kulesekaran, P., Hebda, P. A. and Wells, A. (2008). ELR-negative CXC chemokine CXCL11 (IP-9/ITAC) facilitates dermal and epidermal maturation during wound repair. *Am. J. Pathol.* **173**, 643-652.